Carbohydrate Polymers 107 (2014) 158–166

Contents lists available at ScienceDirect

Carbohydrate Polymers

journal homepage: www.elsevier.com/locate/carbpol

Chitosan-sheath and chitin-core nanowhiskers

Antonio G.B. Pereira [a,b], Edvani C. Muniz [a], You-Lo Hsieh [b,*]

[a] Grupo de Materiais Poliméricos e Compósitos (GMPC) - Department of Chemistry, Maringá State University, Av. Colombo, 5790, Maringá, Paraná 87020-900, Brazil
[b] Fiber and Polymer Science, University of California, Davis, One Shields Avenue, Davis, California 95616, USA

ARTICLE INFO

Article history:
Received 3 August 2013
Received in revised form 12 February 2014
Accepted 14 February 2014
Available online 25 February 2014

Keywords:
Nanowhiskers
Chitin
Chitosan
Deacetylation
Surface modification

ABSTRACT

Chitosan-sheath and α-chitin-core nanowhiskers (CsNWs) have been successfully generated by surface deacetylation of chitin nanowhiskers (CtNWs) in the never-dried state. Acid hydrolysis (3N HCl, 30 mL/g, 104 °C) of pure chitin derived from crab shell yielded 65% 4–10 nm thick, 16 nm wide and 214 nm long chitin whiskers (CtNWs) that were 86% crystalline and 81% acetylated. Surface deacetylation of CtNWs was robust in their never-dried state in 50% NaOH at a moderate 50 °C for 6 h, yielding 92% CsNWs. All deacetylated CsNWs retain the same α-chitin crystalline core at reduced 50% crystallinity and similar dimensions (4–12 nm thick, 15 nm wide, 247 long) as CtNWs, but reduced 60% acetylation reflecting the deacetylated surface layers. Progressive surface deacetylation was evident by the increased IP as well as increased positive charges under acidic pH and reduced negative charges at alkaline pH with increasing reaction time.

1. Introduction

Chitin, a β(1 ⟶ 4)-linked *N*-acetyl-β-D-glucosamine polysaccharide (Percot et al., 2002), is a structural component in the exoskeletons or cell walls (Tharanathan & Kittur, 2003) of arthropods, nematodes and fungi (Rinaudo, 2006). Chitin is highly crystalline and has been shown to exist in three polymorphic forms: α (the most common with antiparallel chain alignment), β (parallel chain alignment) and γ (the least common of two parallel alternate with one antiparallel chain) (Merzendorfer, 2006). In the native form, chitin chains assemble spontaneously into 2–5 nm wide and 300 nm long nanofibrils, each comprising ca. 25 molecules, which are organized into larger 50–300 nm wide fibrils, with some variations associated to the sources (Raabe et al., 2005). Acid hydrolysis has yielded crystalline chitin nanorods, commonly referred as nanowhiskers, by differential removal of amorphous domains of chitin (Marchessault et al., 1959; Paillet & Dufresne, 2001), that are a few tens of nanometer in diameters and 150 nm up to 2 μm in lengths, depending on sources and hydrolysis conditions (Zeng et al., 2011).

Chitin nanowhiskers (CtNWs) have been used to improve properties of other polymers. Incorporating 30 wt% of CtNWs in gel spun polyvinyl alcohol (PVA) fibers improved their Young's modulus from 28 GPa to 50 GPa (Uddin et al., 2012). Coating a very thin 0.1 μm layer of CtNWs to 25 μm thick poly(lactic acid) (PLA) film could substantially decrease its O_2 permeability by 180 times (Fan et al., 2012). Adding 50 wt% CtNWs in sodium alginate (SA) microspheres increased their swelling in pH 7.4 phosphate buffer from 1815% to 2329% (Lin et al., 2011). CtNWs have also been surface modified by reacting the hydroxyl groups with phenyl isocyanate, alkenyl succinic anhydride and 3-isopropenyl-α,α′-dimethylbenzyl isocyanate (Gopalan Nair et al., 2003), but these modified surfaces did not enhance the mechanical properties of CtNWs-rubber composites for which they were intended.

Chitin can be easily deacetylated into chitosan whose primary amine groups exhibit cationic polyelectrolyte behavior in acidic aqueous medium as well as mucoadhesivety, antibacterial and antifungal biological activities, desirable for many applications (Dash et al., 2011; Rabea et al., 2003; Rinaudo, 2006; Shukla et al., 2013). Efforts to deacetylate CtNWs to date have shown to destroy the original crystalline structure or the nanowhisker form. Deacetylating CtNWs in 40 wt% NaOH solution under different lengths of time (14–28 h) and temperatures (100–180 °C) increase the degree of deacetylation (DD) with increasing reaction times and temperatures, reaching a maximum of 98% DD after 14 h at 180 °C or 18 h at 150 °C (Phongying, Aiba, & Chirachanchai, 2006, 2007). Under these conditions, the crystalline CtNWs were turned into amorphous fibrillar porous structure, indicating deacetylation of the CtNWs bulk. Microwave-assisted alkaline hydrolysis of CtNWs has shown

* Corresponding author. Tel.: +1 5307520843; fax: +1 5307527584.
E-mail address: ylhsieh@ucdavis.edu (Y.-L. Hsieh).

http://dx.doi.org/10.1016/j.carbpol.2014.02.046
0144-8617/

to reach 80% and 95% deacetylation in 40 and 60 wt% NaOH, respectively, after for 6 h (Lertwattanaseri et al., 2009), also loosing the nanowhisker morphology. It is clear that these deacetylation conditions are too harsh and have deacetylated their bulk, destroying the desirable crystalline structure.

This study was aimed to produce isolated chitosan nanowhiskers (CsNWs) by deacetylating only the surfaces of CtNWs while retaining the crystalline core. Pure chitin was to be isolated from crab shell chitin and hydrolyzed to CtNWs by HCl. Deacetylation of CtNWs by NaOH was systematically studied under different conditions of temperatures and/or reaction times to hydrolyze the nanowhisker surfaces while preserving the crystalline core. Controlling reaction temperature and time was deemed paramount to reach the balance between effective deacetylation on the surfaces while retaining the highly crystalline bulk. The chitosan amine functional surfaces and crystalline chitin core of CsNWs present attractive surface-core combination of nanowhiskers for potentially improved applications as reinforcement in polymeric nanocomposites and for formation of aerogels, liquid crystal system, among others.

2. Materials and methods

2.1. Materials

Chitin from crab shells (CAS 1398-61-4) was purchased from Sigma (St Louis, MO, USA). Potassium hydroxide (85%, EM Science, CAS 1310-58-3), sodium hydroxide (97%, EMD, CAS 1310-73-2), hydrochloric acid (36.5%, EMD, CAS 7647-01-0), pH 4 acetate buffer (15% sodium acetate and 48% acetic acid, VWR), sodium chlorite (80%, Alfa Aesar, CAS 7758-19-2) were used without further purification. Purified water (Millipore-Milli-Q™ Water System) was used in all experiments. All aqueous solutions were prepared in % unless specified.

2.1.1. Chitin purification and whiskers

Crab shell chitin was purified by removing residual proteins and color impurities following a previous procedure (Paillet & Dufresne, 2001). Proteins were removed by stirring 5 g of chitin in 150 mL of 5% KOH aqueous solution at boil for 6 h, then at room temperature for another 12 h, filtered and washed with water. The solid was bleached in 150 mL of 1.7% $NaClO_2$ in pH 4 acetate buffer at 80 °C for 2 h, filtered, then bleached again under the same condition for another 2 h, filtered and washed with water. The solid material was re-suspended in 150 mL of 5% KOH for 48 h and centrifuged. The purified chitin was washed, then oven dried (50 °C) and weighed to determine yield.

Chitin whiskers (CtNWs) were prepared by hydrolyzing the purified chitin with 3N HCl at boil under stirring for 90 min. The ratio HCl solution/chitin was ca. 30 mL/1 g. The suspension was diluted by adding 50 mL of water and centrifuged at 3400 rpm for 15 min. The precipitate was recovered and re-suspended in 200 mL of water and centrifuged. This process was performed three times. The precipitate was recovered and re-suspended in water and dialyzed until neutral pH. The suspension was adjusted to pH 3 with 1N HCl and sonicated (Misonix, ultrasonic liquid processors, model CL5, USA) for 5 min four times with 5 min pause between sonications followed by centrifugation at 3000 rpm for 10 min for removing any remaining precipitate. The suspension was either kept at 8 °C or freeze-dried (Labconco, USA) at −50 °C for 2 days when necessary. The yield of chitin whiskers was determined gravimetrically.

2.1.2. Chitosan whiskers

Chitosan whiskers (CsNWs) were obtained by the deacetylation of chitin nanocrystals with 50% NaOH aqueous solution at varying temperatures for different lengths of time (Table 1). Following deacetylation, the suspension was diluted with water and centrifuged at 5000 rpm for 10 min, then the supernatant decanted. This process was repeated three times. The samples were dialyzed in water to reach neutral pH, adjusted to pH 3 by 1N HCl, then homogenized by sonication.

Table 1
Deacetylation of CtNWs with 50% NaOH under different conditions.

Condition	Chitin/NaOH (g/100 mL)	Time (h)	Temperature (°C)	Yield (%)	Chitin whiskers condition
1	1.8 (0.5% $NaBH_4$)	0.5	120	89	Freeze-dried
2	0.414	0.5	120	61	Suspension, never-dried[a]
		6		92	Suspension, never-dried[a]
3	0.414	24	50	94	
		48		74	

[a] 1.38 wt-%.

2.2. Characterization

Characterization of CtNWs was performed on never-dried suspension, freeze-dried or air-dried samples. Zeta potential measurements were performed on suspensions of never-dried nanowhiskers. FTIR, XRD, SEM, TGA and DSC were performed on freeze-dried samples whereas suspensions were air-dried on appropriate surfaces for AFM and TEM analysis. Freeze drying of CtNWs or CsNWs suspensions was performed by freezing in liquid nitrogen (ca. −196 °C) and freeze-dried for 3 days (−48 °C and 0.12 mbar, Labconco Free zone dry system, USA).

2.2.1. Zeta potential

Zeta potential measurements were performed on a ZetaSizer (nano ZS90, Malvern) coupled to a autotitrator device (MPT-2). Both CtNW and CsNW suspensions were diluted to 0.1% and the pH was adjusted to ca. 1 by 1N HCl. Zeta potential was measured over the pH range from 1 to 12 using 0.5N NaOH as the titrant.

2.2.2. Fourier transform infra-red spectroscopy (FTIR)

The FTIR spectra of freeze-dried samples pressed with KBr were collected over 64 scans in a Nicolet 6700 FTIR spectrophotometer (Thermo Electron Corporation) operated in the 4000–400 cm^{-1} region at 4 cm^{-1} resolution.

2.2.3. X-ray diffraction (XRD)

XRD spectra were collected on a Scintag XDS 2000 powder diffractometer using a Ni-filtered Cu Kα radiation (λ = 1.5406 Å) at an 45 kV anode voltage and a 40 mA current. Freeze-dried samples were pressed between two glass slides into 1-mm thick flat sheets. XRD patterns were recorded from $2\theta = 5°$ to $2\theta = 40°$ at a scan rate of 2°/min. The XRD data were smoothed using 10 points in a second-order regression based on Savitzky–Golay filter. The crystallinity Index (CrI) was calculated as:

$$\mathrm{CrI} = \frac{A_c}{A_T} \times 100 \quad (1)$$

where, A_c is the total crystalline diffraction peak area, and A_T is the amorphous area under the curve $2\theta = 5°$ to 30°. The XRD patterns were then deconvoluted based on Gaussian or Lorentzian functions in the Origin software release 8.5 to resolve the individual

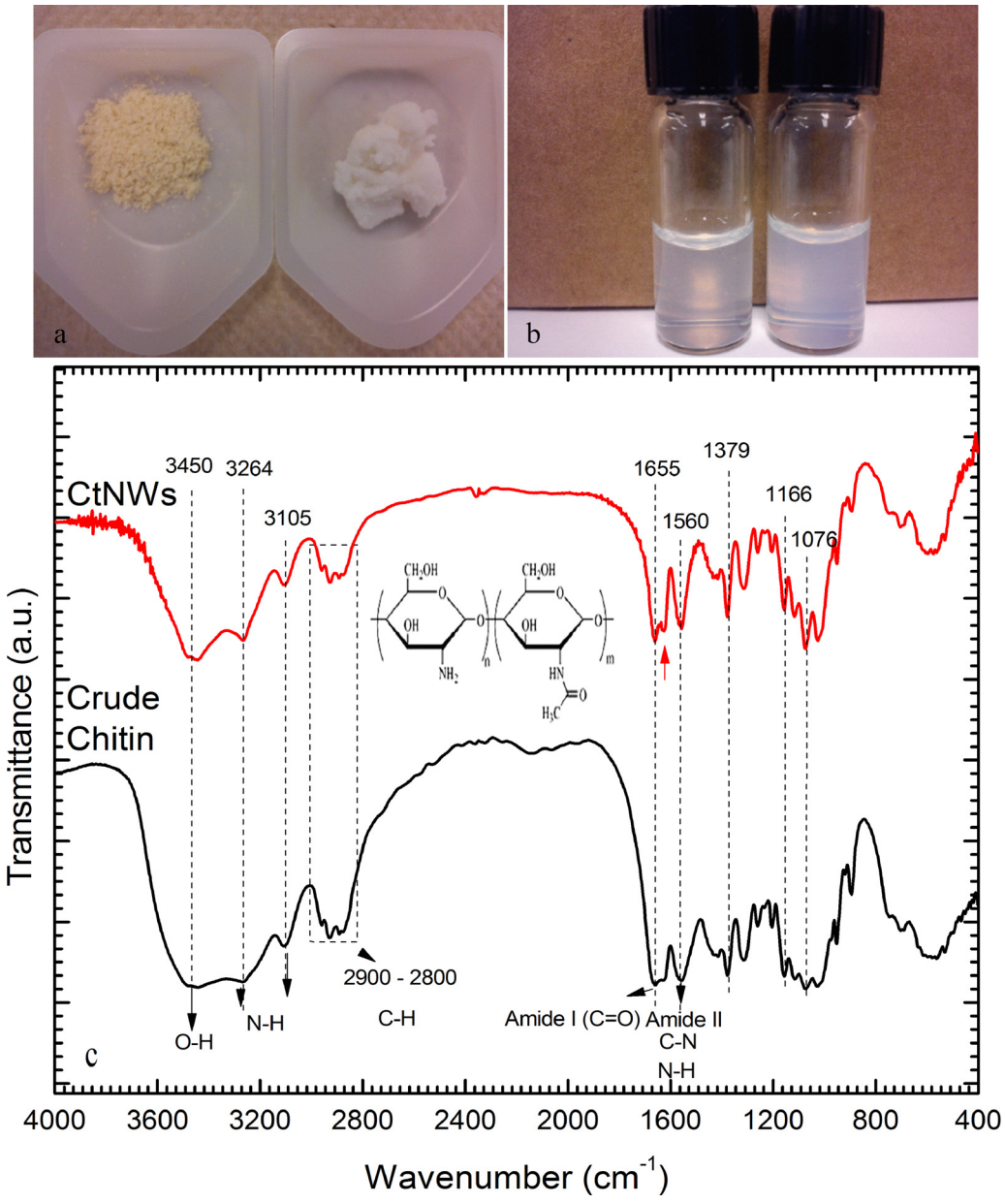

Fig. 1. Chitin purification and HCl hydrolysis: (a) crude (left) and purified (right) chitin; (b) 0.2% (left) and 0.7% (right) CtNWs suspensions (pH 3); (c) FTIR of freeze-dried CtNWs.

peaks. The crystallite size was estimated using the Scherrer's Eq. (2) (Goodrich & Winter, 2006):

$$D_{hkl} = 0.9\lambda\beta_{1/2}\cos\theta \quad (2)$$

where, D_{hkl} is the crystal dimension perpendicular to the diffraction plane with *hkl* Miller indices, λ is the X-ray radiation wavenumber ($\lambda = 0.154$ nm), and $\beta_{1/2}$ is the full width at half maximum (FWHM) of diffraction peak (Fan et al., 2012).

2.2.4. Scanning electron microscopy (SEM)

Freeze-dried samples were sputter gold coated and imaged using a field emission scanning electron microscope (FE-SEM) (XL 30-SFEG, FEI/Philips, USA) at a 5 mm working distance and a 5-kV accelerating voltage.

2.2.5. Thermogravimetric analysis (TGA) and differential scanning calorimetry (DSC)

DSC and TGA of freeze-dried CtNWs and deacetylated CtNWs (method 3) were performed from 30 °C to 550 °C at a 10 °C/min heating rate under flowing N_2 (30 mL/min for DSC and 50 mL/min for TGA) in a DSC-60 differential scanning calorimeter and TGA-50 thermogravimetry analyzer (Shimadzu), respectively.

2.2.6. Atomic force microscopy (AFM)

10 μL of 0.001% CtNWs or CsNWs suspension pH 3 was deposited into a freshly clipped mica substrate and air dried before image acquisition using an Asylum Research Atomic Force Microscope.

2.2.7. Transmission electron microscopy (TEM)

CtNW and deacetylated CtNW samples were prepared by depositing 8 μL 0.01% suspensions onto glow-discharged

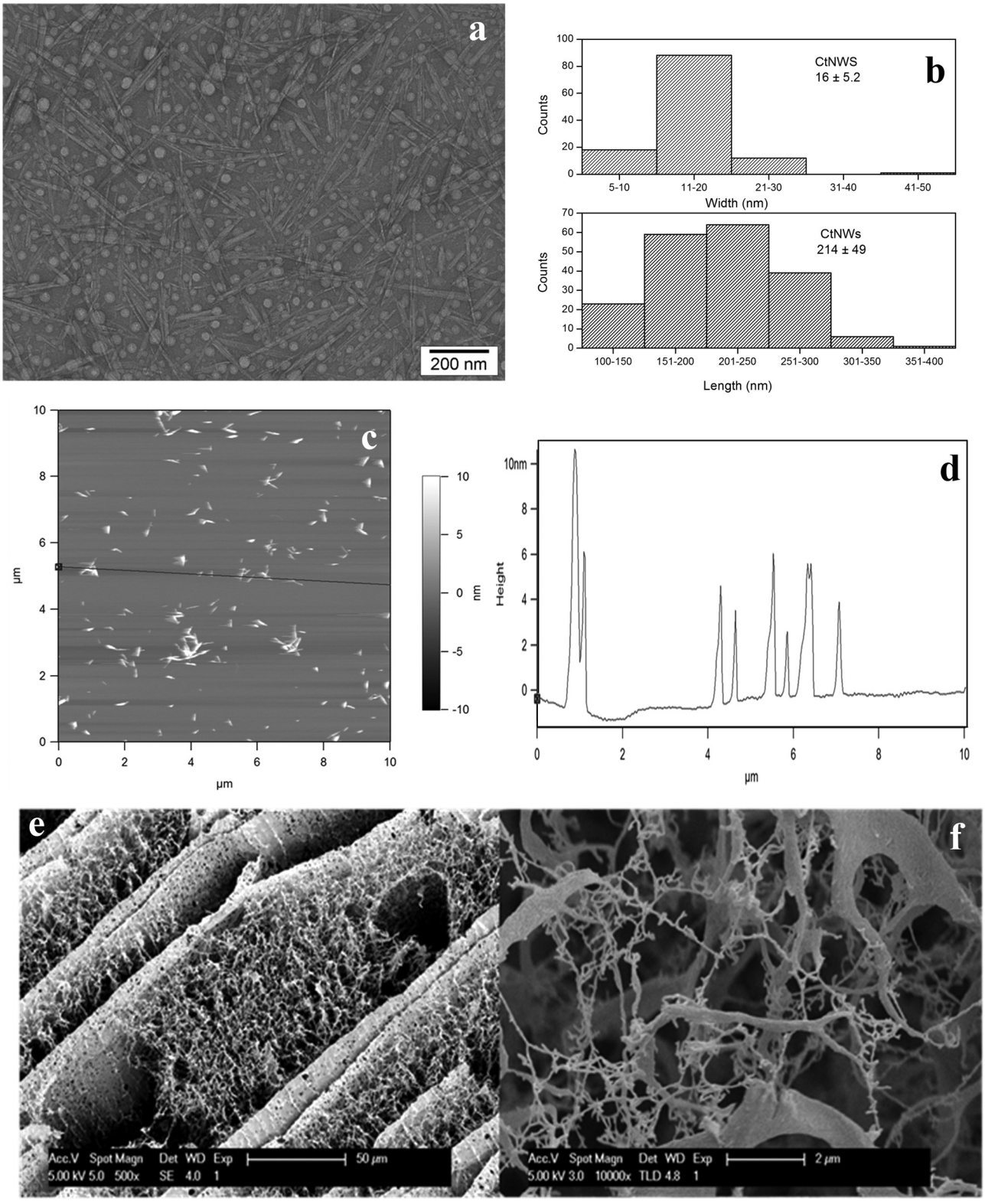

Fig. 2. CtNWs: (a) TEM; (b) width and length distribution profile; (c) AFM height image (d); AFM height profile for line shown in c. (e) and (f) SEM of freeze-dried sample.

carbon-coated TEM grids (300-mesh copper, formvar-carbon, Ted Pella Inc., Redding, CA), and any excess liquid was removed by blotting with a filter paper. The specimens were then negatively stained with 2% uranyl acetate solution for 5 min, blotted with a filter paper to remove excess staining solution and allowed to dry under the ambient condition. The samples were observed using a Philips CM12 transmission electron microscope operating at 100 kV accelerating voltage. The widths and lengths of nanocrystals were collected and the averages were calculated from measurements over 200 samples using analySIS FIVE software.

3. Results and discussion

Pure chitin was obtained by removing proteins (5% KOH, at boil for 2 h, then ambient 12 h) and the yellow-brownish color (1.7% $NaClO_2$, pH 4, 80 °C, 4 h) from crude crab shell chitin to white powders at a 75% yield (Fig. 1a). Acid hydrolysis (3N HCl, 30 mL/g, at boil for 90 min) of pure chitin yielded 65% chitin nanowhiskers (CtNWs), or 48.8% of the original crude crab shell chitin. Hydrochloric acid accesses the amorphous regions to cleave chitin chains to soluble fragments to isolate the crystalline domains. The 35% mass loss from acid hydrolysis was slightly less than the 40% mass loss reported under a similar condition but 30 min longer time (3N HCl, 20 mL/g, 104 °C, 2 h) (Revol & Marchessault, 1993). Aqueous CtNWs suspensions at either 0.2 or 0.7% appeared slightly translucent (Fig. 1b), showing the hydroxyl and acetylamide groups on the whisker surfaces to be sufficiently polar to keep the whiskers separated and afloat. This appearance is similar to chitin suspensions at same pH (ca. 3) reported by others (Fan et al., 2010). FTIR of CtNWs exhibited absorption peaks characteristic of chitin, i.e., O—H stretching at 3450 cm^{-1}, N—H stretching at 3264 cm^{-1} and 3105 cm^{-1}, C—H vibrations in the 2900–2800 cm^{-1} range, amide I C=O at 1655 cm^{-1}, amide II (a combination of C—N—H stretching and N—H bending) at 1560 cm^{-1} and C—N stretching at 1166 cm^{-1} (Fig. 1c). The shoulder at 1655 cm^{-1} is due to intermolecular hydrogen bondings between acetylamide groups (C—O···H—N) and intramolecular hydrogen bonding between acetylamide C=O and C6 hydroxyl OH, reported to be associated only with α-chitin (Lavall et al., 2007; Rinaudo, 2006), indicating CtNWs to be α-chitin. The sharper peaks in the CtNWs spectrum than those of crude chitin are attributed to its higher chitin purity and crystallinity. These FTIR data confirm that the acid hydrolysis did not alter the chemical nature nor α-chitin form of CtNWs from crude chitin, as expected.

TEM images of CtNWs show their widths to range from 5 nm to 30 nm with an 16 nm average and their lengths from 100 nm to 350 nm with an 214 nm average, or a 13 length-to-width aspect ratio (Fig. 2a,b). The AFM height profile shows CtNWs to vary from 4 nm to 10 nm, similar to the lower range for widths shown in TEM (Fig. 2d). The AFM image also showed large size variations among CtNWs (Fig. 2c). However, lateral dimensions observed in AFM are not as accurate as those derived from TEM due to possible tip broadening effect.

The SEM images (Fig. 2e,f) of rapidly frozen and freeze-dried CtNWs show them to self-assemble into tens of micron thick sheet-like layers with much smaller sub-micron fibrillated network structures in between. Deacetylation conducted on freeze-dried CtNWs (50% NaOH, 120 °C, 0.5 h, condition 1 in Table 1) produced clusters of larger particles rather than individual whiskers even at an elevated temperature. In light of losing individual nanowhisker form to this bulky assembled structure from freeze drying, deacetylation was performed on never-dried CtNW sample, shown as deacetylation condition 2.

Indeed deacetylation (50% NaOH, 120 °C, 0.5 h) of CtNWs in the never-dried state, i.e., condition 2, produced individually isolated rod-shape nanowhiskers (Fig. 3a). The AFM height profile showed similar height distribution ranging from 4 nm to 12 nm as the original CtNWs. The yield was ca. 60% however, relatively low possibly due to hydrolysis of smaller CtNWs into soluble oligomers.

To reduce possible cleavage of the chitin backbone during deacetylation, the reaction was conducted at a much lower 50 °C, but longer time from 6 h to 48 h (condition 3 in Table 1). The yield was clearly improved to ca. 74% for the 48 h deacetylation reaction and to 92% and 94% yields for the 6 h and 24 h reactions, respectively. The appearance of deacetylated CtNWs suspensions is quite similar to the original CtNWs suspension, suggesting a good dispersibility in aqueous media. In all cases, CtNWs deacetylated for 6, 24 and 48 h show the same rod-shape morphology that is independent of the lengths of deacetylation time and as the original CtNWs (Fig. 3). Therefore, the optimal yield of deacetylated CtNWs in the never-dried state was achieved for 6 h of reaction with 50% NaOH at 50 °C.

The AFM phase images show smaller and more numerous CsNWs with increasing reaction times, but height profiles are similarly varied from 1 nm to 8 nm in thickness. From TEM images, the average width of CsNWs 48 h derived is 15 ± 5.4 nm, comparable to CtNWs, while the average length is 247 ± 88 nm, broadly distributed (Fig. 4). Most importantly, deacetylation at a moderate temperature of 50 °C over significantly wide range of time did not affect, statistically, neither the average width nor the average length of the nanowhiskers although the average aspect ratio increased slightly to 16. The lower yield at 48 h reaction suggests the loss to more deacetylated chitosan chains and/or smaller nanowhiskers while similar 92–94% yields from the 6 and 24 h reactions suggest mainly surface reactions within 24 h.

FTIR spectra (Fig. 5a) for CsNWs deacetylated from CtNWs for 6 h, 24 h and 48 h are essentially the same as that of CtNWs, showing no observable effects of deacetylation or reaction time. Commercial chitosan, in which most C2 acetylamide groups are converted to amine groups, presented similar vibrational modes of CtNWs with exception of the amide II band at 1560 cm^{-1}. Deacetylation of chitin in the bulk is expected to show some decreasing or disappearance of bands associated with amide groups at 1560 cm^{-1} (C—N—H and N—H) and 1655 cm^{-1} (C=O, primary amide). Using the degree of

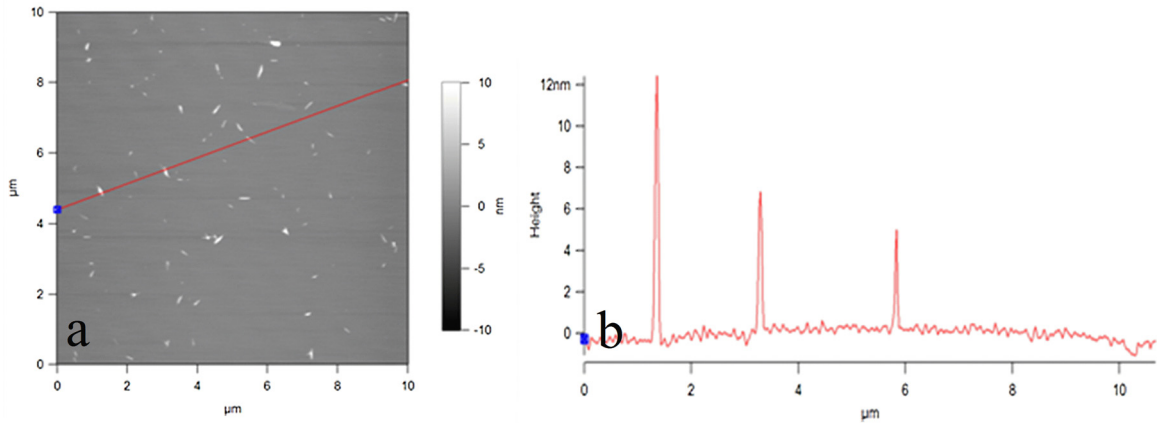

Fig. 3. AFM of CsNWs (deacetylation condition 2, 50% NaOH, 120 °C, 0.5 h): (a) height image; (b) height profile (line shown a).

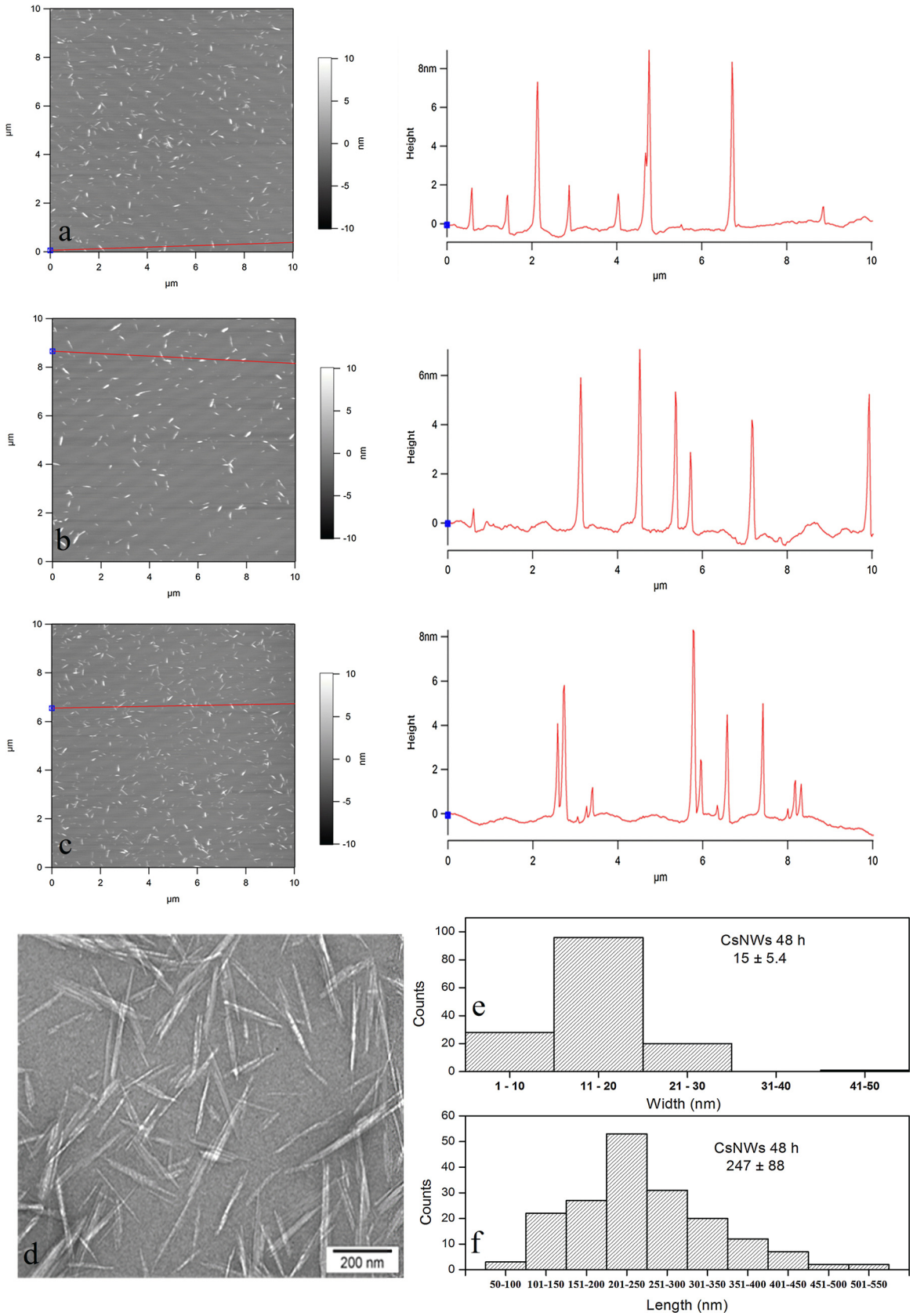

Fig. 4. AFM phase images (left) and height profiles (right) of CsNWs deacetylated (50% NaOH, 50 °C) for: (a) 6 h; (b) 24 h and (c) 48 h; (d) TEM (d) and width (e) and length (f) distribution of CsNWs 48 h.

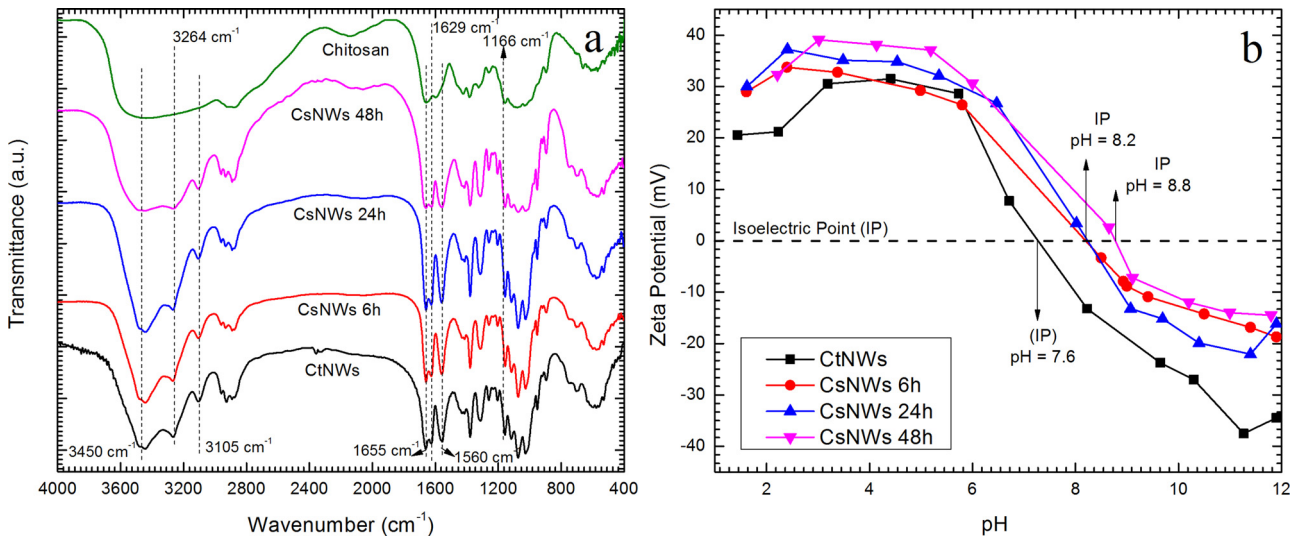

Fig. 5. CtNWs and CsNWs hydrolyzed in 50% NaOH, 50 °C for 6, 24 and 48 h: (a) FTIR spectra; (b) Zeta potential at 0.1% concentration with isoelectric point (IP) indicated.

acetylation (%DA) proposed by Baxter et al. (Baxter et al., 1992), the absorbance ratio at 1655 cm^{-1} (C=O) and 3450 cm^{-1} (A_{1655}/A_{3450}) was calculated to derive %DA follows:

$$\%DA = \left(\frac{A_{1655}}{A_{3450}}\right) \times 115 \quad (3)$$

The DA calculated by Eq. (3) is 84% for crude chitin, 81% for CtNWs and ca. 60% for all three CsNWs, independent of the lengths of deacetylation.

Crude chitin is expected to be less than 100% deacetyalted due to the likely partial hydrolysis in NaOH used to extract proteins.

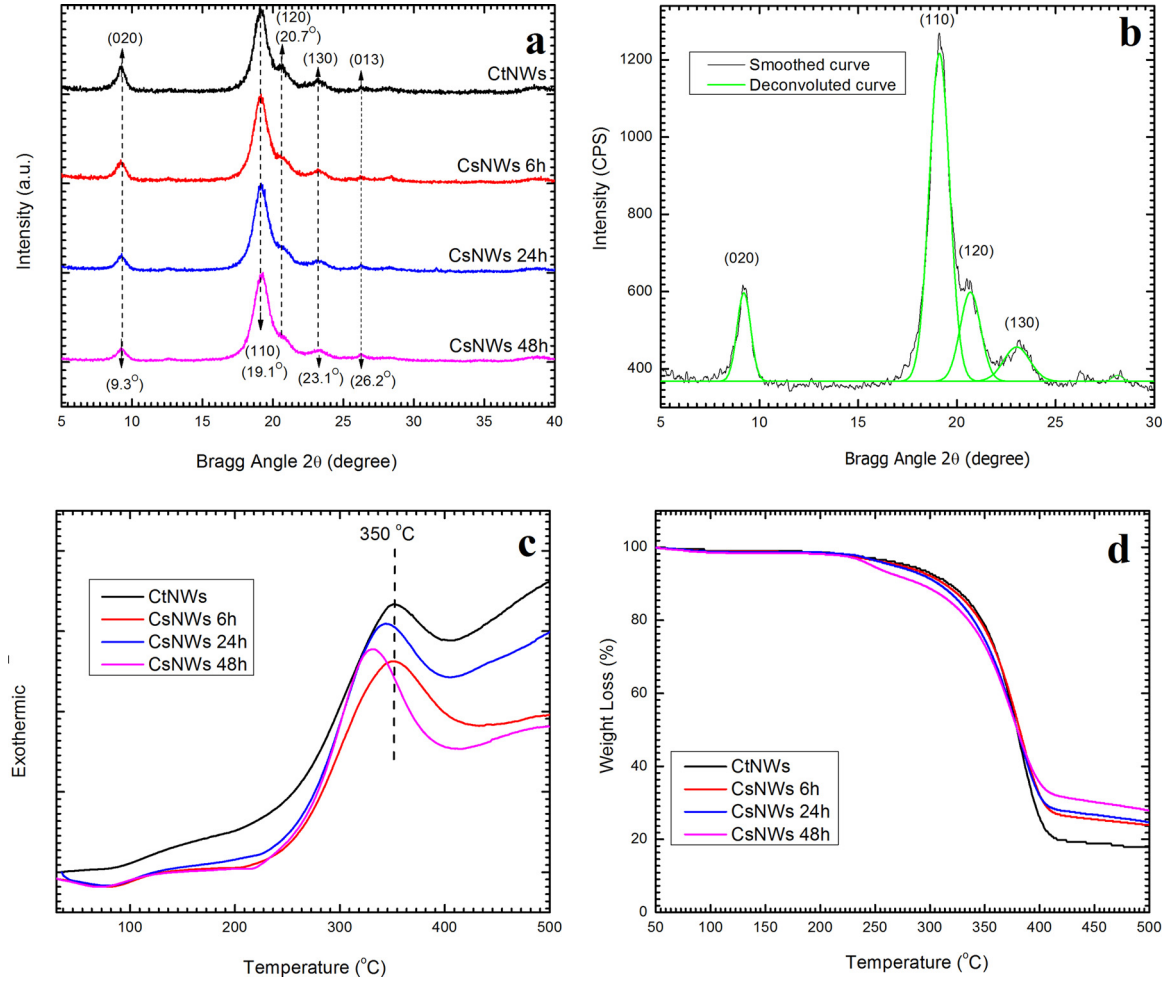

Fig. 6. CtNWs and CsNWs from deacetylation (50% NaOH, 50 °C) for 6 h, 24 h and 48 h: (a) XRD patterns; (b) Deconvolution of CtNWs XRD; (c) DSC and (d) TGA.

Table 2
Crystalline structure of CtNWs and CsNWs deacetylated by method 3.

Sample	Crystallinity index (%)	Crystallite dimension at (0 2 0) plane(nm)	Crystallite dimension at (1 1 0) plane(nm)
CtNWs	86	9.2	6.5
CsNWs 6 h[a]	47	9.1	6
CsNWs 24 h[a]	51	9.7	5.8
CsNWs 48 h[a]	54	10.3	5.5

[a] Deacetylation reaction time.

The harsh acid hydrolysis (3N HCl at boil, 90 min) of pure chitin to CtNWs only cause a very small 3% decrease in DA for CtNWs. Deacetylation under a relatively mild condition (50% NaOH, 50 °C), however, cause a 21% drop in DA for all CsNWs, irrespective of lengths of reaction time. This similarly decreased DA further confirms the reaction time-independent surface effect of deacetylation, i.e., occurring on the surface layer leaving the chitin core unaffected. This is another confirmation of surface deacetylation of CtNWs to chitosan surface and chitin core nanowhiskers or CsNWs.

CtNWs as well as CsNWs deacetylated in 50% NaOH at 50 °C at varying lengths of time all have positive zeta potential values under acidic conditions (Fig. 5b). At pH 3 to 6, CtNWs exhibited ca. 30 mV positive charges and remain as stable aqueous suspensions. At pH below 3, the positive charges reduced to around 20 mV and the suspensions became unstable and began to precipitate, possibly due to the excess of counter-ions in the electrical double layer leading to neutralization of the electrostatic repulsion among CtNWs. As pH increased to above 6, the zeta potential of CtNWs decreased as the amino groups deprotonated. The isoelectric point (IP) where the zeta potential is zero and the colloidal system is least stable was observed at pH 7.6. At pH >7.6, the zeta potential became increasing negative, reaching a maximum of ca. −40 mV at pH 12. This may be due to the associated OH^- from NaOH titrant in the slipping plane of the colloid.

The zeta potential profiles over pH presented similar trends among CsNWs deacetylated for different lengths of time. The most deacetylated CsNWs 48 h are more highly positively charged under acidic pHs but less negatively charged at more basic pHs. The IP also raised to higher pH with longer deacetylation, i.e., from pH 7.6 for CtNWs to pH 8.2 for CsNWs 6 h and CsNWs 24 h then to pH 8.8 for CsNWs 48 h, approaching the pK_a of 9.5 of primary amines ($R-NH_3^+ + H_2O \leftrightarrow R-NH_2 + H_3O^+$) (Lansalot et al., 2003). Fully acetylated CtNWs would present a different zeta potential profile in acidic media due to the absence of amine groups to be protonated and generate positive charges. Therefore, the positive zeta potential clearly indicates CtNWs to be partially deacetylated, consistent with the 84% DA derived from FTIR. The zeta potential profiles, i.e., magnitude (in acidic medium) increasing with reaction times gave clear evidences that acetylamide groups were increasingly converted to amine. This confirms that longer 24 h deacetylation gave rise to more extensive surface reaction while at the similar over 90% yield as the 6 h reaction. Most importantly, this surface charge characterization by zeta potential not only further confirms the successful deacetylation of CsNWs, but also is more sensitive to show surface changes from the extent of reaction. The increasing IP as well as increasing positive charges under acidic pH and reducing negative charges at alkaline pH show progressive deacetylation on the surfaces with time.

The normalized XRD patterns over the 5–30° 2θ for CtNWs and deacetylated CtNWs show refraction peaks located at 2θ = 9.3°, 19.1°, 20.7°, 23.1° and 26.2°, associated with (0 2 0), (1 1 0), (1 2 0), (1 3 0) and (0 1 3) crystallographic planes of α-chitin, respectively (Fig. 6a), and are consistent to those reported by others (Goodrich & Winter, 2006; Minke & Blackwell, 1978). Deacetylation reduced the intensities of most signals and especially at 2θ = 9.3°. All XRD curves were smoothed and deconvoluted to resolve the individual peaks at correlation coefficients (R^2) of 0.99 or higher as exemplified by the deconvoluted curve of CtNWs shown in Fig. 6b. The crystallinity decreases from 86% for CtNWs to ca. 50% for deacetylated CsNWs (Table 2). The crystallite dimensions at (0 2 0) and (1 1 0) planes for CtNWs are 9.2 nm and 6.5 nm, respectively, consistent with those observed previously (Fan et al., 2010). The crystallite size, at (0 2 0) planes, did not change by deacetylation for 6 h, but slightly increased with longer deacetylation times of 24 h and 48 h. On the other hand, at (1 1 0) plane the crystallite dimension decreased slightly with longer reaction time. Such small variations in the crystallite dimensions corroborates with zeta potential and FTIR data suggesting the deacetylation happens preferentially on the surfaces rather than the bulk.

CtNWs show mainly one thermal transition associated to degradation beginning at above 200 °C and peaked at 350 °C (Fig. 6c). All three CsNWs show small endothermic transition around 80 °C, related to the evaporation of bounded water. This small change is consistent with both the more hydrophilic nature of CsNWs and the surface effects of deacetylation. The degradation peaks also lower to 343 °C and 330 °C for CsNW 24 h and CsNW 48H, respectively, showing CtNWs to be slightly more thermally stable than CsNWs and the longest deacetyaled CsNWs 48 h to be least stable (Fig. 6d).

It is clear that deacetylation did not significantly alter neither the rod-like morphology nor nanowhisker dimensions, but induced more surface changes with increasing reaction time in the form of increasing IP points, higher positive charges at acidic condition and lower negative charges under basic conditions, decreased crystallinity and lower thermal stability. These findings show successful surface deacetylation of CtNWs in 50% NaOH at a moderate 50 °C to chitosan-surface and chitin-core CsNWs. The chitin core remains similar while the chitosan surface varied by the length of deacetylation reaction time.

4. Conclusion

This paper reports robust and efficient derivation of chitosan-sheath and α-chitin core nanowhiskers or CsNWs. Pure chitin was isolated from crab shell chitin by removing proteins (5% KOH, at boil, 18 h) and bleaching (1.7% $NaClO_2$, pH 4, 80 °C, 4 h) with 84% degree of acetylation (DA) and 75% yield. Acid hydrolysis (3N HCl, 30 mL/g, 104 °C) of pure chitin yielded 65% crystalline (86% CrI) and slightly deacetylated (81% DA) chitin whiskers (CtNWs) that were 4–10 nm thick, 16 nm wide and 214 nm long on the average with ca. 13 length-to-width aspect ratio. Surface deacetylation of CtNWs was optimal in their never-dried state in 50% NaOH at a moderate 50 °C for 6 h, yielding 92% CsNWs. Irrespective of reaction time, all surface deacetylated CsNWs had similar dimensions (4–12 nm thick, 15 ± 5.4 nm wide, 247 ± 88 nm long) with a 16 aspect ratio as well as reduced 50% CrI and 60% DA, confirming surface deacetylation of CtNWs to chitosan surface and chitin core nanowhiskers or CsNWs. While all CsNWs had similar extent of α-chitin cores, progressive deacetylation occurring in the surface layers was evident by the increased IP as well as increased positive charges under acidic pH and reduced negative charges at alkaline pH with increasing reaction time. These chitosan surface and crystalline α-chitin core CsNWs successfully derived have uniquely

pH-dependent charged and reactive surfaces, highly crystalline core and nanometric dimensions to be highly versatile shealth-core nanomaterials. These chitosan shealth and crystalline α-chitin core CsNWs have the advantage of being derived from a greatly available natural polymer. Their unique combination of shealth and core characteristics is versatile for broad applications, including surface modifying agents, self-assembling nanomaterials, fillers for composites, among others.

Acknowledgment

A.G.B. Pereira is very grateful to Dr. F. Jiang for the assistance on TEM, SEM and XRD and to CAPES for the doctorate's fellowship (Process BEX 2394/11-1) as a visiting scholar at University of California, Davis.

References

Baxter, A., Dillon, M., Anthony Taylor, K. D., & Roberts, G. A. F. (1992). Improved method for i.r. determination of the degree of *N*-acetylation of chitosan. *International Journal of Biological Macromolecules*, *14*(3), 166–169.

Dash, M., Chiellini, F., Ottenbrite, R. M., & Chiellini, E. (2011). Chitosan—A versatile semi-synthetic polymer in biomedical applications. *Progress in Polymer Science*, *36*(8), 981–1014.

Fan, Y., Fukuzumi, H., Saito, T., & Isogai, A. (2012). Comparative characterization of aqueous dispersions and cast films of different chitin nanowhiskers/nanofibers. *International Journal of Biological Macromolecules*, *50*(1), 69–76.

Fan, Y., Saito, T., & Isogai, A. (2010). Individual chitin nano-whiskers prepared from partially deacetylated α-chitin by fibril surface cationization. *Carbohydrate Polymers*, *79*(4), 1046–1051.

Goodrich, J. D., & Winter, W. T. (2006). α-Chitin nanocrystals prepared from shrimp shells and their specific surface area measurement. *Biomacromolecules*, *8*(1), 252–257.

Gopalan Nair, K., Dufresne, A., Gandini, A., & Belgacem, M. N. (2003). Crab shell chitin whiskers reinforced natural rubber nanocomposites. 3. Effect of chemical modification of chitin whiskers. *Biomacromolecules*, *4*(6), 1835–1842.

Lansalot, M., Elaissari, A., & Mondain-Monval, O. (2003). *Polymer colloids*. New York: Marcel Dekker.

Lavall, R. L., Assis, O. B. G., & Campana-Filho, S. P. (2007). β-Chitin from the pens of *Loligo* sp.: Extraction and characterization. *Bioresource Technology*, *98*(13), 2465–2472.

Lertwattanaseri, T., Ichikawa, N., Mizoguchi, T., Tanaka, Y., & Chirachanchai, S. (2009). Microwave technique for efficient deacetylation of chitin nanowhiskers to a chitosan nanoscaffold. *Carbohydrate Research*, *344*(3), 331–335.

Lin, N., Huang, J., Chang, P. R., Feng, L., & Yu, J. (2011). Effect of polysaccharide nanocrystals on structure, properties, and drug release kinetics of alginate-based microspheres. *Colloids and Surfaces B: Biointerfaces*, *85*(2), 270–279.

Marchessault, R. H., Morehead, F. F., & Walter, N. M. (1959). Liquid crystal systems from Fibrillar Polysaccharides. *Nature*, *184*, 632–633.

Merzendorfer, H. (2006). Insect chitin synthases: A review. *Journal of Comparative Physiology B*, *176*(1), 1–15.

Minke, R., & Blackwell, J. (1978). The structure of α-chitin. *Journal of Molecular Biology*, *120*(2), 167–181.

Paillet, M., & Dufresne, A. (2001). Chitin whisker reinforced thermoplastic nanocomposites. *Macromolecules*, *34*(19), 6527–6530.

Percot, A., Viton, C., & Domard, A. (2002). Optimization of chitin extraction from shrimp shells. *Biomacromolecules*, *4*(1), 12–18.

Phongying, S., Aiba, S.-i., & Chirachanchai, S. (2006). A novel soft and cotton-like chitosan-sugar nanoscaffold. *Biopolymers*, *83*(3), 280–288.

Phongying, S., Aiba, S.-i., & Chirachanchai, S. (2007). Direct chitosan nanoscaffold formation via chitin whiskers. *Polymer*, *48*(1), 393–400.

Raabe, D., Sachs, C., & Romano, P. (2005). The crustacean exoskeleton as an example of a structurally and mechanically graded biological nanocomposite material. *Acta Materialia*, *53*(15), 4281–4292, ialia.

Rabea, E. I., Badawy, M. E. T., Stevens, C. V., Smagghe, G., & Steurbaut, W. (2003). Chitosan as antimicrobial agent: Applications and mode of action. *Biomacromolecules*, *4*(6), 1457–1465.

Revol, J. F., & Marchessault, R. H. (1993). In vitro chiral nematic ordering of chitin crystallites. *International Journal of Biological Macromolecules*, *15*(6), 329–335.

Rinaudo, M. (2006). Chitin and chitosan: Properties and applications. *Progress in Polymer Science*, *31*(7), 603–632.

Shukla, S. K., Mishra, A. K., Arotiba, O. A., & Mamba, B. B. (2013). Chitosan-based nanomaterials: A state-of-the-art review. *International Journal of Biological Macromolecules*, *59*(0), 46–58.

Tharanathan, R. N., & Kittur, F. S. (2003). Chitin—The undisputed biomolecule of great potential. *Critical Reviews in Food Science and Nutrition*, *43*(1), 61–87.

Uddin, A. J., Fujie, M., Sembo, S., & Gotoh, Y. (2012). Outstanding reinforcing effect of highly oriented chitin whiskers in PVA nanocomposites. *Carbohydrate Polymers*, *87*(1), 799–805.

Zeng, J.-B., He, Y.-S., Li, S.-L., & Wang, Y.-Z. (2011). Chitin whiskers: An overview. *Biomacromolecules*, *13*(1), 1–11.